Validation of Astec2.1 using Quench-12 for VVER-Reactors

Ahmet Kağan Mercan *, Victor Hugo Sánchez-Espinoza, Fabrizio Gabrielli

Karlsruhe Institute of Technology (KIT), Institute for Neutron Physics and Reactor Technology (INR), Hermann-von-Helmholtz-Platz 1, 76344 Eggenstein-Leopoldshafen, Germany

ARTICLE INFO

Keywords:
QUENCH-12
ASTEC
LOCA
VVER
Validation

ABSTRACT

Russian VVER-type reactors are one of the most common used commercial reactors in the world. The validation of severe accident codes using experimental data is focused in core degradation both in-vessel and ex-vessel phenomena such as the QUENCH-12 tests performed at the Karlsruhe Institute of Technology (KIT). This step is needed before integral codes are applied to evaluate the behavior of VVER-plants under severe accident conditions. The main goal of the QUENCH-12 test was to evaluate the hydrogen generation resulting from the injection of cold quench water into an overheated and oxidized bundle of fuel rod simulators representing the VVER-fuel rods. Such phenomena are expected to occur during a severe accident sequence e.g. LOCA or as part of an accident management measure. This paper describes the investigations done to simulate the QUENCH-12 test using the ASTEC V2, which is developed by IRSN to simulate all physical and chemical phenomena during severe accident condition. A model of the QUENCH-12 test facility was developed for ASTEC first time taking into account the specific material data, geometry and boundary conditions. The evaluation of the results have shown, that ASTEC V2 is able to predict the main trends of key-parameters during the all test phases in good agreement with the measured data. The integral hydrogen generation is only over-predicted during the quench phase. As next steps, the model will be improved by taking into account the real material properties of the ZrNb-cladding typical of Russian reactors instead of the ones of Zr. Also the sensitivity studies regarding the electrical heater resistance will be carried out.

1. Introduction

After nuclear accidents (like Three Mile Island, Chernobyl and Fukushima), safety-related investigations have shown that both SAM-measures and severe accident codes must be improved and optimized. Another major outcome was the need off enhance the defense-in-depht (DiD) concept in nuclear power plants to assure the mitigation of severe accidents (OECD/NEA, 2013). Furthermore, NEA member countries conducted stress tests for all nuclear power plants with the focus on design-basis accidents and beyond-design-basis-accident situations (OECD/NEA, 2013). Indeed, many countries and regulators started to investigate severe accident cases for their own reactors to ensure public health, to enhance safety barriers and public health. Regulators implemented action plans for the implementation of necessary measures and severe accident management and they implemented new safety analysis and new concepts including stopping or delaying severe accident cases (BMUB, 2012; BMUB, 2014; Kymäläinen et al., 1997). Since VVER type reactors are being built in different places of the world, it is important to assess the safety features of this type of reactor and their behavior under severe accident conditions. In addition, the determination of hydrogen generation, oxidation and material relocation for VVER specified materials is of great importance when discussing concepts for severe accident management (SAM). Finally, benchmark activities has been started to assess the predictions capabilities of severe accident codes such as MAAP, MELCOR, ATHLET-CD/COCOSYS, and ASTEC regarding the estimation of the radiological source term (OECD/NEA, 2013). Also new benchmark applications are being developed to estimate radiological dispersion inside and outside the reactor pressure vessel (D'Auria et al., 2008; Chatterjee et al., 2011; Gencheva et al., 2015) or containment (Kruse et al., 2014; Gonfiotti and Paci, 2018).

The European severe accident code ASTEC (Accident Source Term Evaluation Code) is being developed to simulate entire severe accident sequence from the initiating state to the release of radioactive material to the environment (Chatelard and Reinka, 2009; Chatelard et al., 2014; Chatelard, 2016). Several projects like SARNET and CESAM are established to enhance capabilities of ASTEC and explore necessary upgrades,

* Corresponding author.
E-mail addresses: ahmet.mercan@partner.kit.edu (A.K. Mercan), victor.sanchez@kit.edu (V.H. Sánchez-Espinoza), fabrizio.gabrielli@kit.edu (F. Gabrielli).

and NUGENIA, MUSA and CAMIVVER projects are being studied for state-of-the-art investigations. To achieve these, several validation and verification projects are implemented (Fichot et al., 2017; Belon et al., 2017; Chatelard et al., 2017)(Gómez-García-Toraño et al., 2017). Currently, ASTEC is being modified for the modelling of spent fuel pools, new reactor designs and fusion facilities (Pietro Maccari, 2021; Coindreau, 2018).

At KIT, the ASTEC-code is being validated for the analysis of VVER-severe accidents in the frame of a doctoral thesis. It will be concentrated on the quantification of the radiological source term using a validated ASTEC–version and the follow-up estimation of the radiological consequences using the KIT-code JRODOS. The first step of this work is the validation of ASTEC-2.1 with the QUENCH-12 experiment representing VVER-fuel rods. The main goal of QUENCH-12 test is to investigate the behavior of overheated VVER-fuel rod bundle which is quenched with cold water. The focus of the investigations is the high-temperature oxidation, the melt formation, relocation as well as the chemo-physical eutectic reactions. The reflooding of the overheated rod bundle leads to steam generation and to the oxidation of hot metallic surfaces in contact with steam e.g. fuel rod cladding, shroud inner surface. As a result of it, hydrogen is generated not only due to the oxidation of the metallic surfaces but also of the molten material containing metals. The accurate prediction of these processes is very important to assess the vulnerability of the containment due to the risk of hydrogen combustion, even detonation, in a nuclear power plant after a severe accident (Henrie and Postma, 1987). However, the injection of cold water into overheated core as an SAM-measure may result in a rapid increase of the temperature and to an enhanced oxidation and hydrogen generation (Sehgal, 2012).

2. Short description of the Quench-12 test

In the frame of the KIT QUENCH test program, the test section was equipped with fuel rod simulators representing the fuel of VVER-reactors. In these tests, behavior during the loss of water inventory in the core, re-flooding of the uncovered cores, generation of hydrogen for different type of claddings and reactor types have been simulated and the main goal of the test program is to generate an extensive database for code development and validation (Seopold, 2001).

The QUENCH-12 test is performed to study the behavior of a VVER-bundle under reflooding conditions and to compare it with the observations done during the QUENCH-06 experiment, which represent fuel rods of western-type PWR (Sepold et al., 2004).

The experimental data gained in QUENCH-12 was also used to validate other codes such as ATHLET-CD and SVECHA/QUENCH (Palagin and Stuckert, 2007; Georgiev and Stuckert, 2012).

2.1. The Quench-12 test section

A vertical cut of the QUENCH-12 test section is shown in Fig. 1. Test bundle is centered in system and surrounded with zirconia fiber insulation. Cooling jacket consists of three sections which are inner cooling jacket, outer cooling jacket and argon cooling between these jackets, and jacket is used as insulation for test bundle. Steam and argon flow from starting at bottom and exits system from upper head which includes mass spectrometer to measure generated hydrogen. Quenching water enters system at bottom section. Main goals of the test are investigation of the oxidation process of cladding during steam flow,which is supported by steam-argon flow in test, and measuring hydrogen generation due to quenching from quenching process.

In Fig. 2, a view of the test section with cooling jacket and insulation is exhibited. There, 13 unheated and 18 heated simulator rods are arranged in triangles as is the case in a real fuel assembly of VVER-reactors. In addition, six corner rods made of Zr-1%Nb (E110) are located at the outer row of the test section to assure similar thermal hydraulic conditions for all rods. The rod pitch is 12.75 mm. and seven

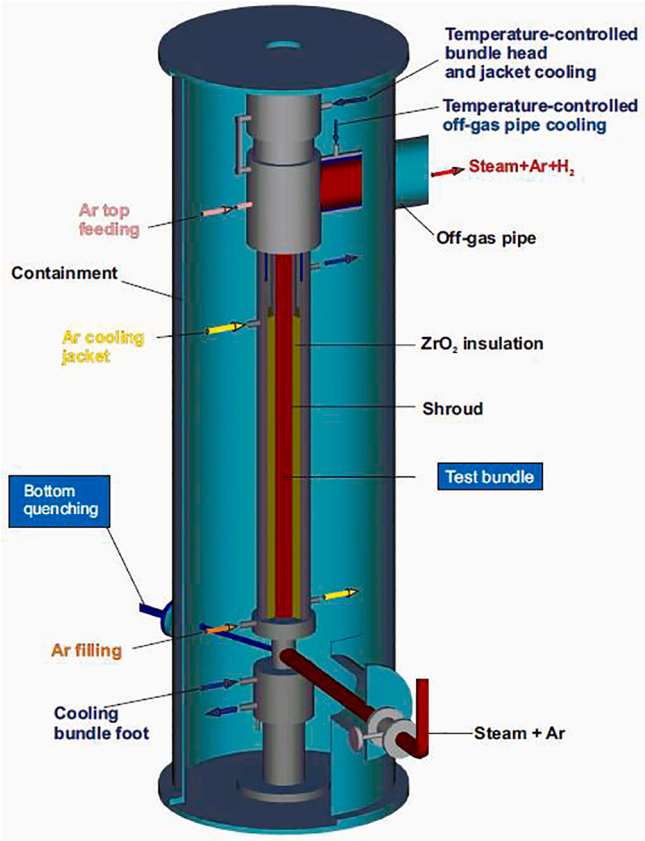

Fig. 1. QUENCH Facility, Containment and Test Section (Stuckert et al., 2008).

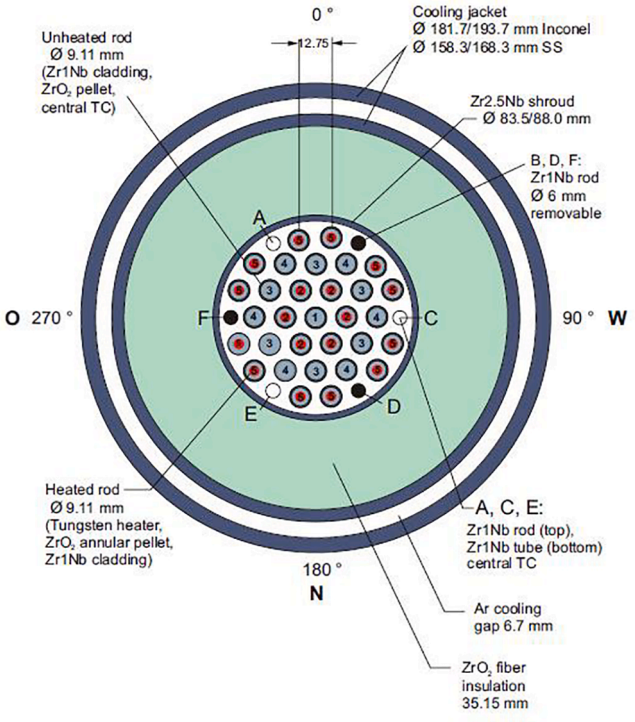

Fig. 2. QUENCH-12 VVER fuel rod simulator bundle (cross section, top view) including rod group numbers (Stuckert et al., 2008).

spacer grids are distributed to hold all simulator rods along the active part. All spacer grids are made of Zr-1%Nb (E110). The heated simulator rods, as seen on Fig. 4., consist of a 4 mm thick tungsten heater, which are connected to molybdenum and copper electrodes at the end of each heated rod. The total heated length is 1024 mm. Instead of fuel pellets, the simulator rods are made of ZrO_2 with a central hole. The bore size of the heated rods is 4.15 mm and 2.5 mm of the unheated rods, see Fig. 5. The Zr-1%Nb (E110) cladding thickness is 0.7 mm. The shroud surrounds the test section and is made of Zr-2.5%Nb (E250). The space between the shroud and the inner cooling jacket cylinder is filled with ZrO_2-fiber. Between the inner and the outer cooling jacket flows argon for cooling purposes. (See Fig. 3)

The initial and boundary conditions used for the ASTEC-simulation were taken from the experimental procedure e.g. the electrical power, steam and argon flow, see Fig. 6. The quenching of the test bundle initiates at 7270 s. The different phases of the test (Stuckert et al., 2008), are listed hereafter:

- **Phase 1: initial phase.** During this phase, the test section is heated for 1.5 h.
- **Phase 2: stabilisation phase.** It lasts for one hour in order to stabilize the bundle at around 600 °C
- **Phase 3: heat-up phase.** During this phase, the electrical heat is increased step by step until 10 kW
- **Phase 4: pre-oxidation phase.** In this phase, oxidation takes place at constant steam flow. At the end of this stage, the corner rod B is ejected from bundle for observation.
- **Phase 5: transient phase.** The electrical power is increased rapidly until 16.6 kW. At the end of this stage, corner rod D is taken out from the test section.
- **Phase 6: quench phase.** The overheated test section is quenched with 48 g/s. The electrical power is decreased to 4 kW, level corresponding to the decay heat.

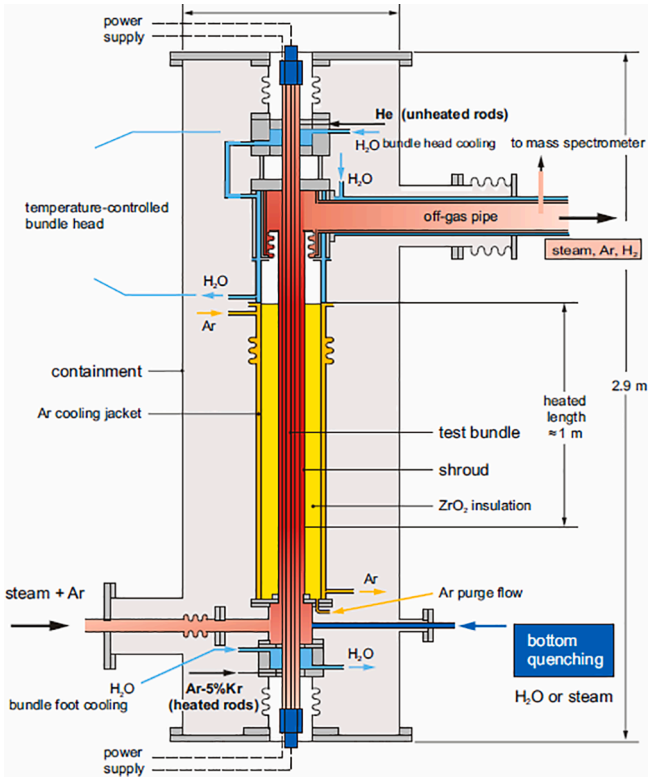

Fig. 3. QUENCH-12 Test Bundle (Stuckert et al., 2008).

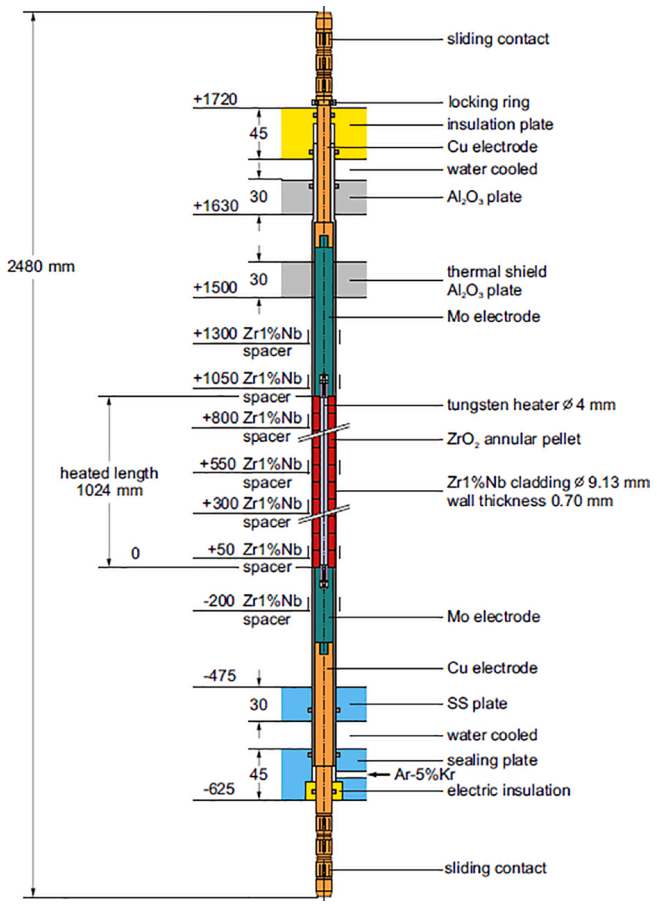

Fig. 4. QUENCH-12 heated rod structure (Stuckert et al., 2008).

2.2. *Quench-12 modelling*

An ASTEC V2.1 model of the QUENCH-12 test includes three fluid channels represent the test section. In the first channel, a central rod (group 1) representing the unheated simulator rod and six heated simulator rods (group 2) are modeled. In Channel 2, 12 unheated simulator rods (group 3 and group 4) are represented and divided into two sections since their radial distances to center is different. In channel 3, six corner rods and 12 heated simulator rods (group 5) are considered, as seen Fig. 7. Since model includes 3 channels, 3 radial meshing are used. Channel 1 is defined between 0 and 24.36 mm, radius of channel 3 is between 24.36 mm and 37.11 mm and between 37.11 and 41.75 mm channel 3 is located.

The materials of the simulator and corner rods are defined according to the ones used in the test. However, Zircaloy-4 is used instead of Zr-1% Nb (E110) for the cladding, corner rods, grid spacers and shroud since ASTEC does not have yet a material databank for VVER-specific materials (Zr-1%Nb (E110) and Zr-%2.5Nb (E250)). In Fig. 8, the isomaterial distribution of the QUENCH-12 test as represented in ASTEC is shown. Model includes 5 main regions at different elevations. Elevations between 0.425 m to 0.3 m is divided 4 meshes and this region has copper as material for heated rods. Between 0.3 to 0 m has molybdenum as material for heated rods and divide 5 meshes. Heated region is between 0 and 1.024 m of experiment and is divided 24 axial meshes. Elevation between 1.024 and 1.3 m is divided 6 meshes and elevation between 1.3 and 1.5 is divided 5 meshes. Heated region has been divided 42.67 mm per mesh.

The ICARE module in ASTEC has been activated to calculate thermophysical changes during the transient. Different sets of models are activated to account for the key-phenomena going on as follows:

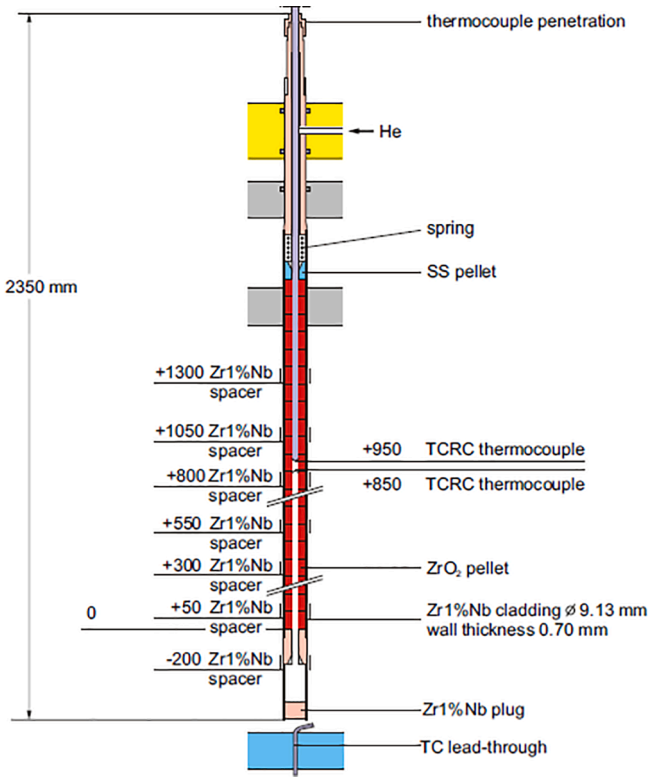

Fig. 5. QUENCH-12 unheated rods and central rod structure (Stuckert et al., 2008).

- Heat conduction:
  - Conduction between ZrO_2 and clad structures are considered. Additionally, heated rods include conduction between electrical heating element and ZrO_2
  - Conduction between shroud and insulation and between insulation and cooling jacket is defined.
  - Spacer grids conduction is defined.
  - Argon at top of insulation region is defined as solid and conduction is modelled according to its convection and radiation heat transfer.
  - Thermal boundary for outer cooling jacket has been used.
- Heat transfer between the rods and the fluid in the test section: DRACCAR code which allows to model thermochemical and mechanical behavior of water-cooled fuel rods.
- Radiation between rods of the different rows in the test section and between the simulator rods and the inner shroud surface are defined.
- Oxidation model: It starts at 600 K and the BEST-FIT correlation is used (Volchek et al., 2004).
- Criterion for loss of integrity of the fuel rod simulators and spacer grids:
  - If the cladding temperature is larger than 2300 K and if the oxide layer thickness is below 300 μm
  - The cladding temperature above 2500 K.

The CESAR module covers thermal–hydraulic behavior in the vessel

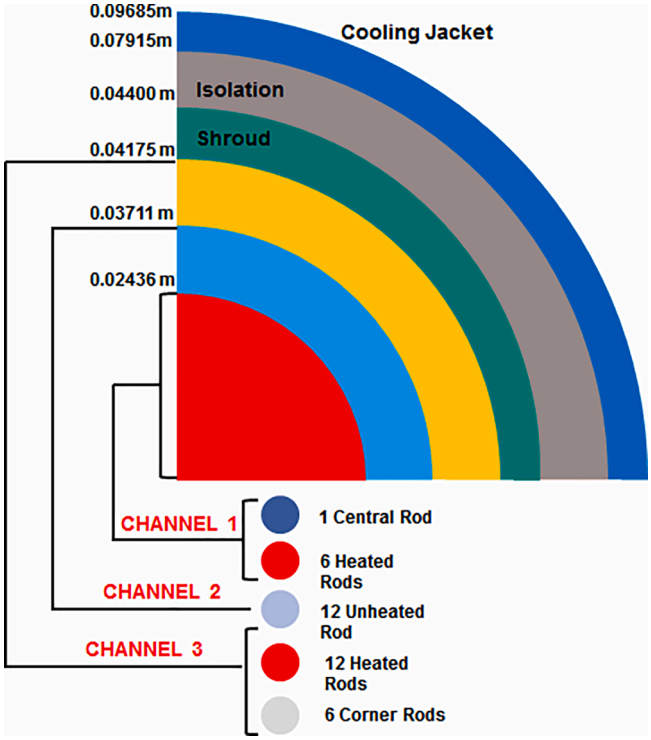

Fig. 7. ASTEC model of QUENCH-12.

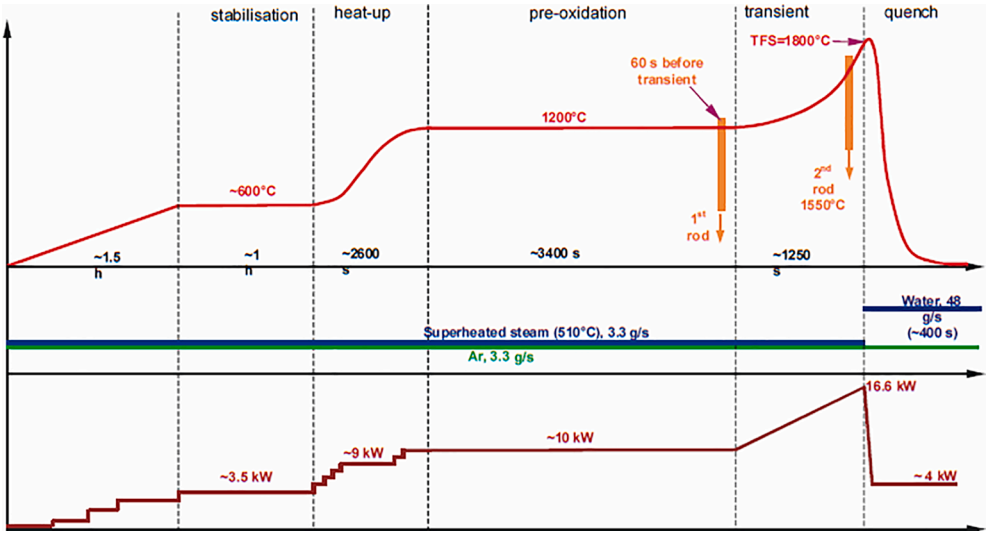

Fig. 6. QUENCH-12 phases and boundary conditions (Stuckert et al., 2008).

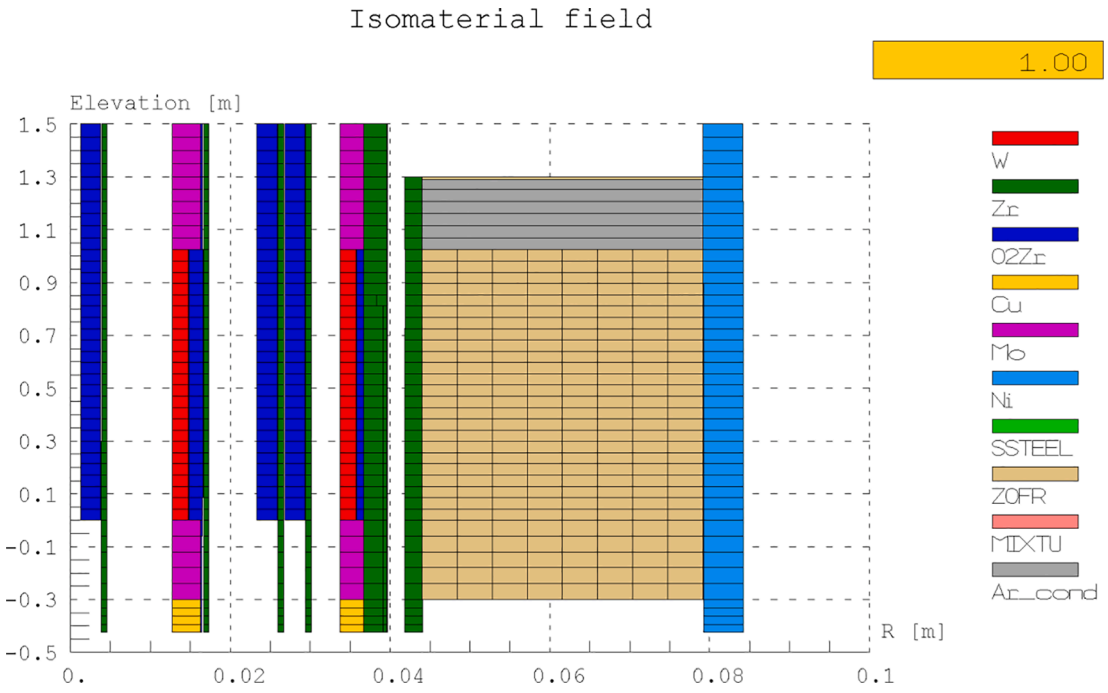

Fig. 8. ASTEC isomaterial field distribution of QUENCH-12.

and primary circuit. The flow of steam and argon has been modelled with this module to represent experiment. Additionally, quench injection has been modelled with CESAR module. The power profile used in the modelling was represented on Fig. 9 and flow inside of the vessel was shown on Fig. 10. The external temperature boundary condition has been used on cooling jacket.

3. Discussion of selected results

In this chapter, selected parameters that predicted by ASTEC V2.1 are compared with the measured data to evaluate the prediction capability of the numerical code. Hence, a short summary of the measured data will be given first.

3.1. Short summary of measured data of the test section

From starting 250 mm to 1350 mm, system is divided 17 elevations with 100 mm array and thermocouples are located in those elevations.

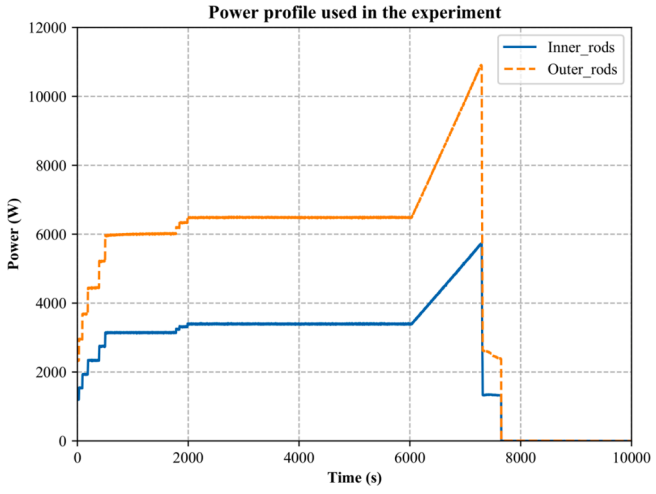

Fig. 9. Established power profile for inner heated rods and outer heated rods.

In the lower bundle region, i.e. up to the 550 mm elevation, NiCr/Ni thermocouples (1 mm diameter, stainless steel sheath 1.4541, MgO insulation) are used for temperature measurement of rod cladding and shroud. The thermocouples of the hot zone are high-temperature thermocouples with W-5Re/W-26Re wires, HfO2 insulation, and a duplex sheath of tantalum (internal)/Zirconium with an outside diameter of 2.1 mm (Stuckert et al., 2008). However not all rods have thermocouples therefore temperature measurements for all rods at every elevation are not possible to use them comparison. Also some of thermocouples are failed before or during experiment. Additionally at every elevation, shroud temperature and cooling jacket temperatures are recorded in experiment.

Hoses for steam, argon and quenching water have flowmeters to measure flow rate of fluent that are used in the bundle. These flowmeters has $\mp$ 0.7 g/s uncertainty. Mass spectrometer is used for measuring produced hydrogen in system. The integration of the hydrogen flux over the annealing time gives the amount of hydrogen extracted from the specimen. Also, a hydrogen detection system located in a bypass to the off-gas line downstream the condenser.

Metallographic examination is done with RIAR (Research Intitute of Atomic Reactors (RIAR), 2019) and FZK (Karlsruhe Institute of Technology (KIT), 2020) institutes. The RIAR and FZK were selected in this way that the bottom ones were investigated at FZK, and the top ones at RIAR. Oxidation of the claddings is estimated by the results of measured thickness of unoxidized claddings layer and the thickness of the formed zirconia and alpha zirconium layers, stabilized by oxygen by using a metallographic microscope (Stuckert et al., 2008).

3.2. ASTEC V2.1 predictions of QUENCH-12 test

From Figs. 11 to 20, the assessment of the predicted and measured cladding temperature in selected time represented. Selected time points are the beginning of transient which is at 6000 s and ejection of second corner rod at 7160 s, respectively. As seen from the figures, the trend is similar between test results and ASTEC estimations. Generally, over predicted temperatures were observed in the result which could lead higher hydrogen estimations. The slight decrease during the calculation was resulted due to spacer grid interaction but the affect was more

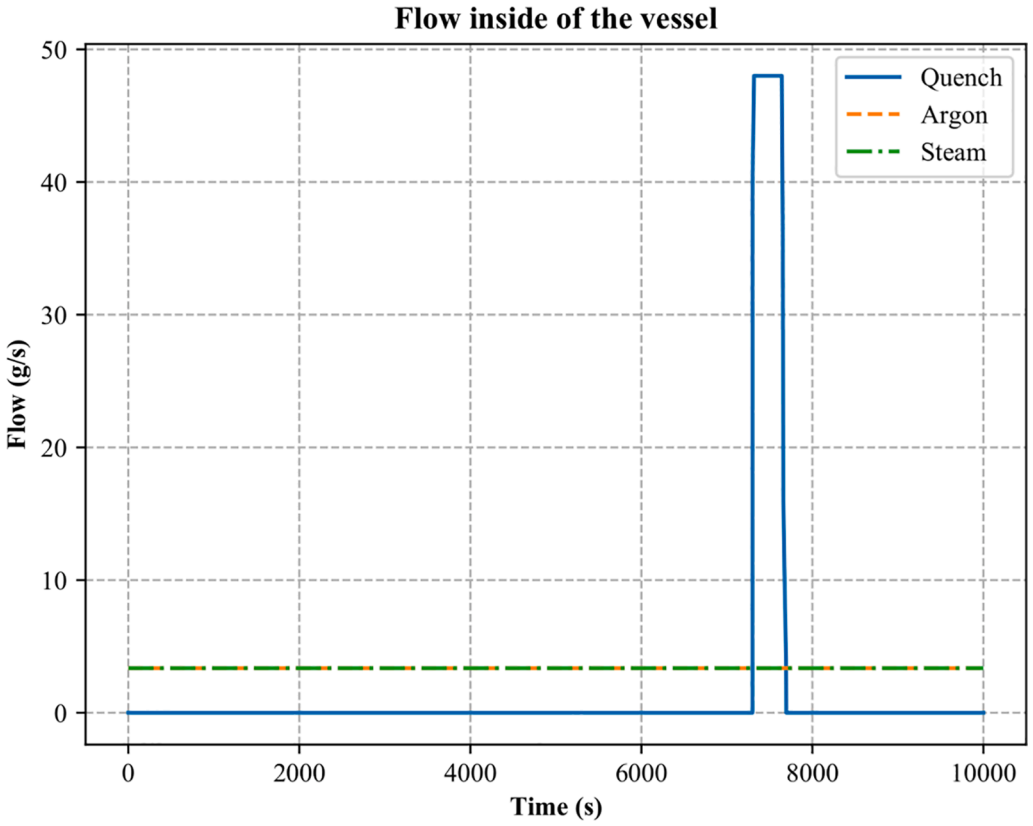

Fig. 10. The steam, argon and quenching water flow rate during the simulation.

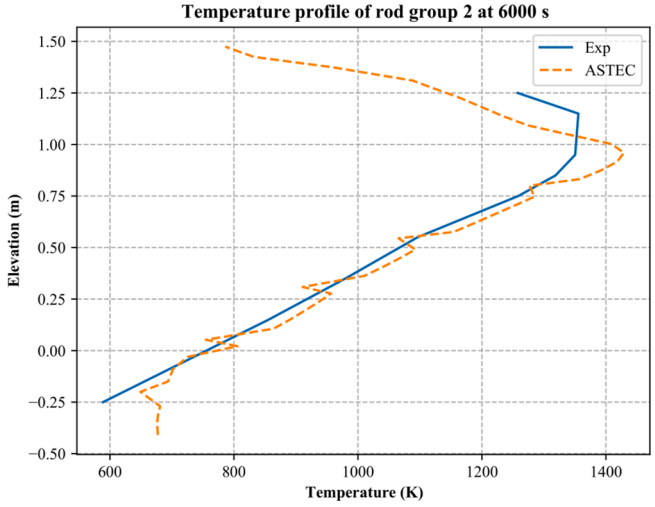

Fig. 11. Temperature profile of cladding temperature of the inner heated rods (rod group 2) (ASTEC) versus experiment (Exp) at 6000 s.

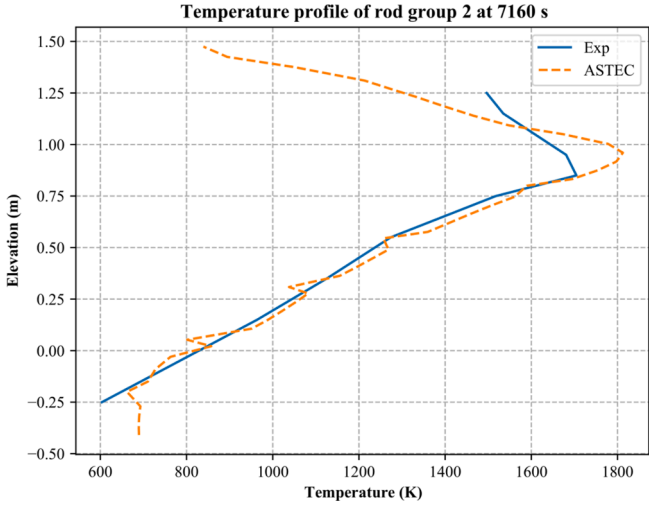

Fig. 12. Temperature profile of cladding temperature of the inner heated rods (rod group 2) (ASTEC) versus experiment (Exp) at 7160 s.

observable at temperatures on the inner rod claddings.

The cladding temperature predicted by ASTEC V2.1 for the heated, unheated and corners rods as well as for the shroud at the elevation of 950 mm is compared to the corresponding measured data. This elevation is the point where highest temperatures are recorded and indication of shroud and clad failures are detected. In Fig. 21and Fig. 22, the comparison of the cladding temperature predicted for the inner heated rod (group 2) and outer unheated rod (group 3) are established with the measured data at 950 mm elevation. The same application is also done in Fig. 23 and Fig. 24 for the comparison of the outer heated rod (group 5) and the shroud temperature predicted and measured at 950 mm elevation. In the test, at around 900 m shroud failure was observed. Also, due to melting process occurred at 950 mm, the experimental temperatures oscillate during the test.

Fig. 25 and Fig. 26 represent oxide scale estimations and results of ejected corner rods at different times. These results are important in order to see how accurate the code estimates the oxide scale. The predictions of the ASTEC code was close to the experiment but higher estimations were observed at 6000 s especially at the highest temperature point. The estimation over the oxide scaled on corner rod at the 7160 s. is really close to the experimental results.

In Fig. 27 and Fig. 28, the total hydrogen generation and the rate of

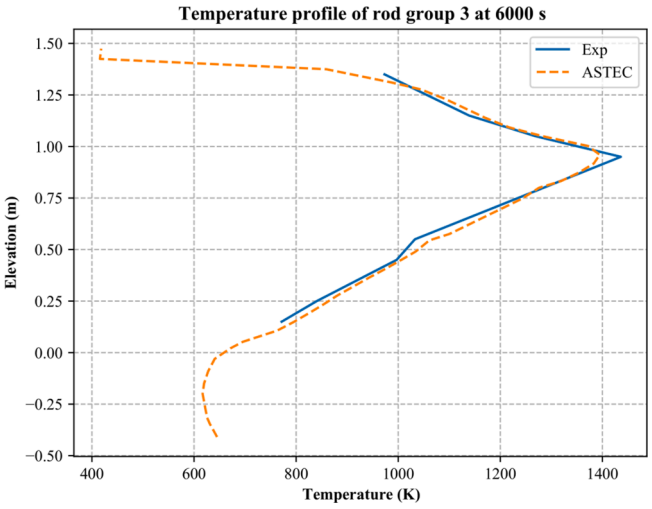

Fig. 13. Temperature profile of cladding temperature of the inner unheated rods (rod group 3) (ASTEC) versus experiment (Exp) at 6000 s.

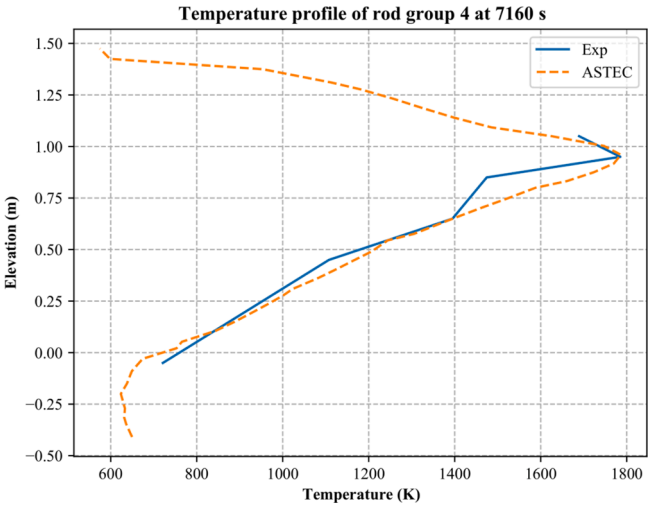

Fig. 16. Temperature profile of cladding temperature of the outer unheated rods (rod group 4) (ASTEC) versus experiment (Exp) at 6000 s.

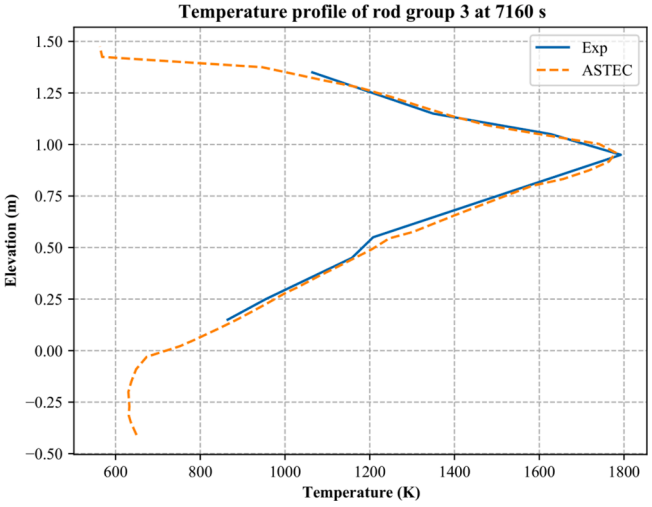

Fig. 14. Temperature profile of cladding temperature of the outer unheated rods (rod group 3) (ASTEC) versus experiment (Exp) at 7160 s.

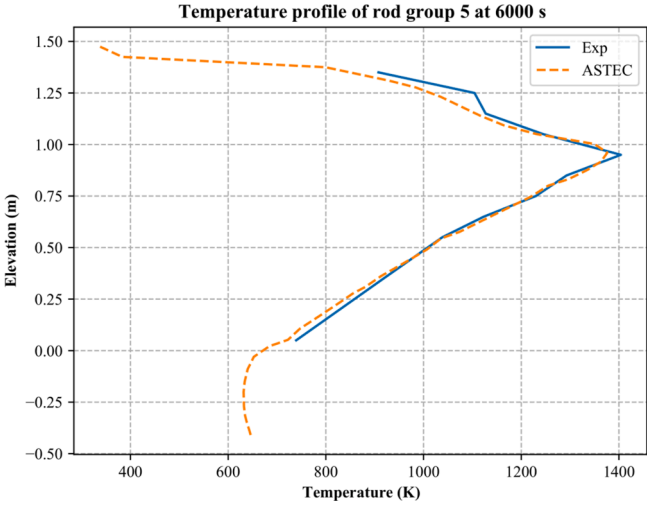

Fig. 17. Temperature profile of cladding temperature of the outer heated rods (rod group 5) (ASTEC) versus experiment (Exp) at 6000 s.

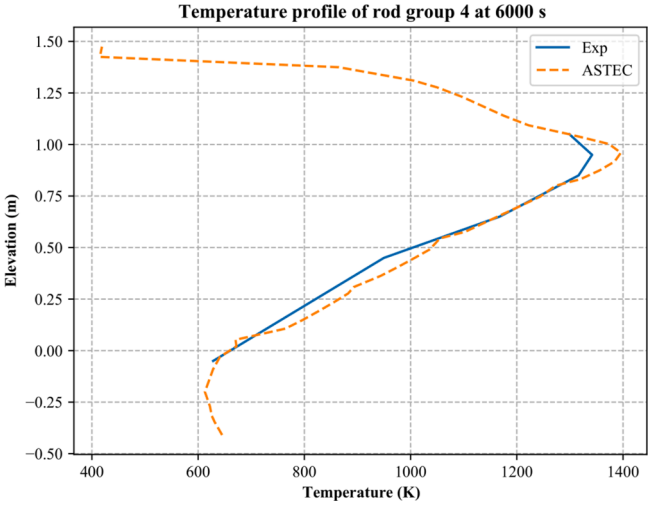

Fig. 15. Temperature profile of cladding temperature of the outer unheated rods (rod group 4) (ASTEC) versus experiment (Exp) at 6000 s.

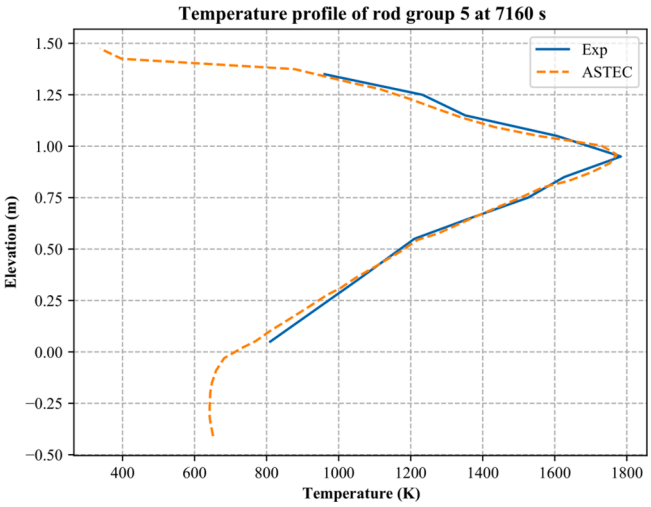

Fig. 18. Temperature profile of cladding temperature of the outer heated rods (rod group 5) (ASTEC) versus experiment (Exp) at 7160 s.

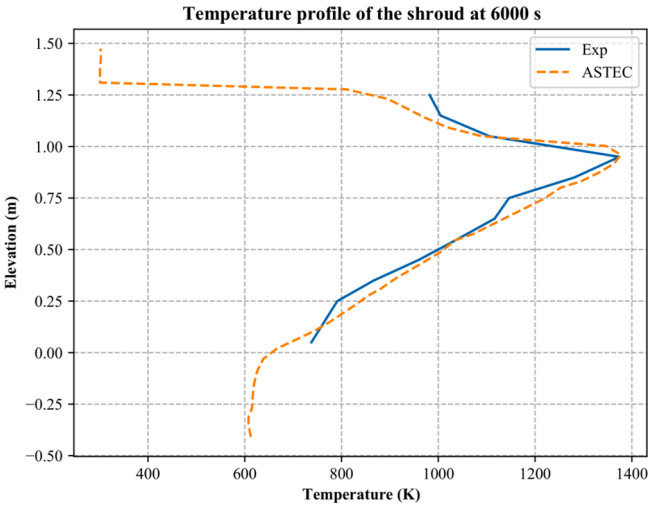

Fig. 19. Temperature profile of the shroud (ASTEC) versus experiment (Exp) at 6000 s.

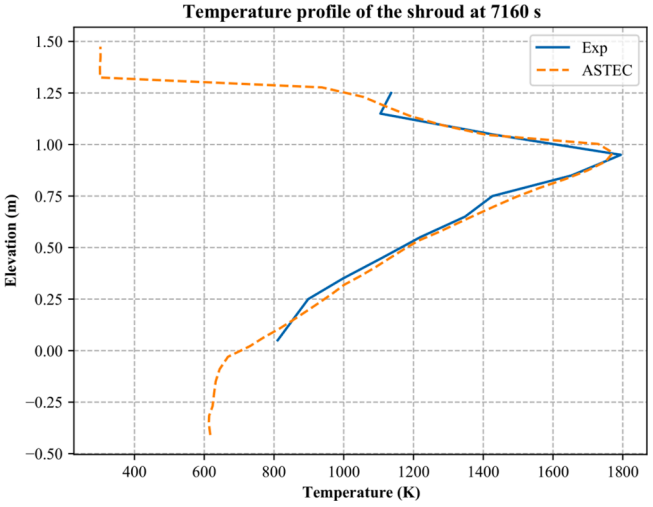

Fig. 20. Temperature profile of the shroud (ASTEC) versus experiment (Exp) at 7160 s.

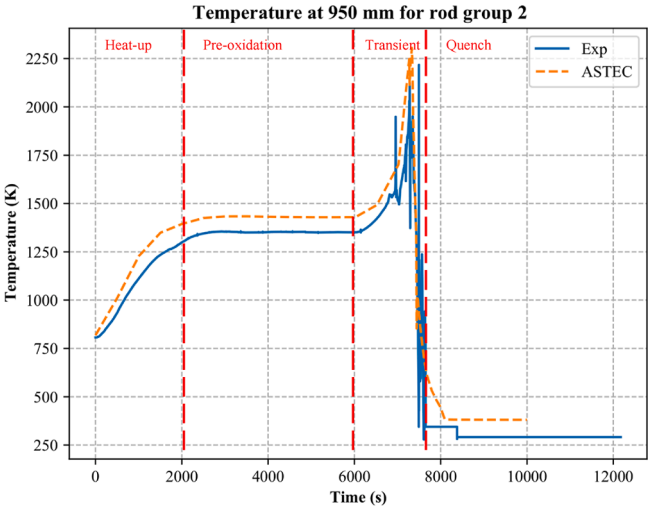

Fig. 21. Measured (Exp) versus predicted (ASTEC) cladding temperature of the inner heated rods at the elevation of 950 mm.

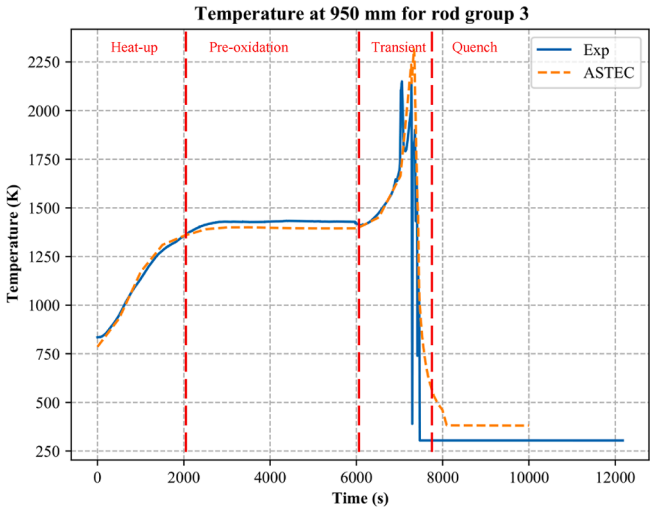

Fig. 22. Measured (Exp) versus predicted (ASTEC) cladding temperature of the outer unheated rods at the elevation of 950 mm.

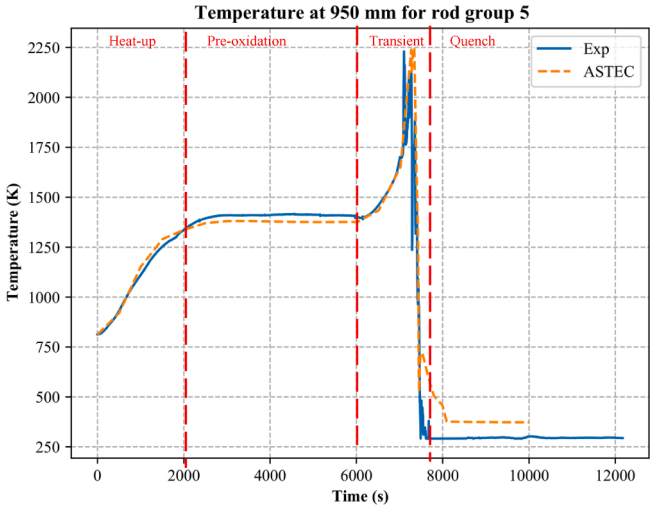

Fig. 23. Measured (Exp) versus predicted (ASTEC) cladding temperature of the outer heated rods at the elevation of 950 mm.

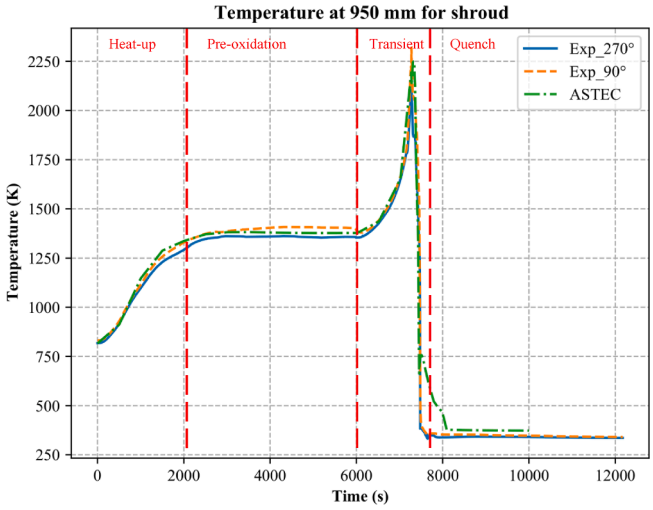

Fig. 24. Measured (Exp) versus predicted (ASTEC) temperature of the shroud at the elevation of 950 mm.

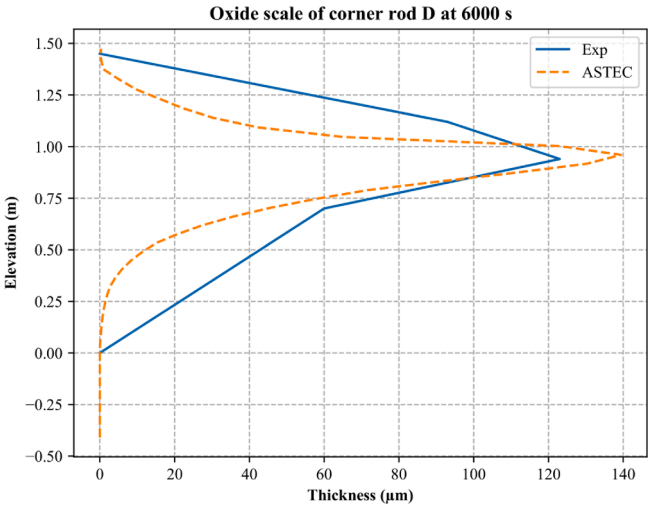

Fig. 25. Measured (Exp) versus predicted (ASTEC) oxide scale results for corner rods.

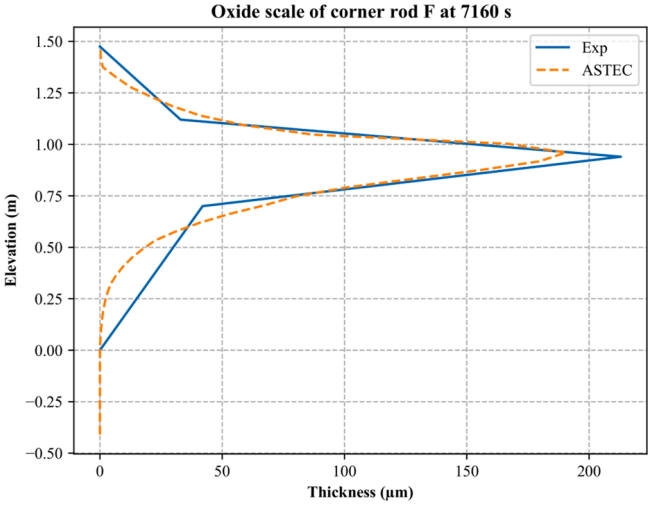

Fig. 26. Measured (Exp) versus predicted (ASTEC) oxide scale results for corner rods.

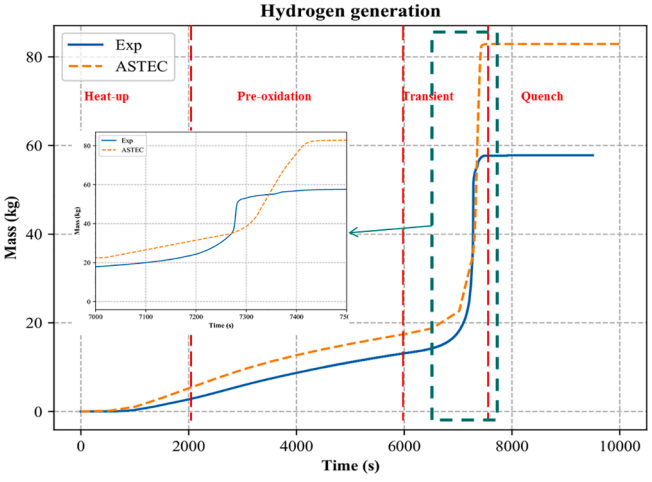

Fig. 27. Hydrogen generation in time.

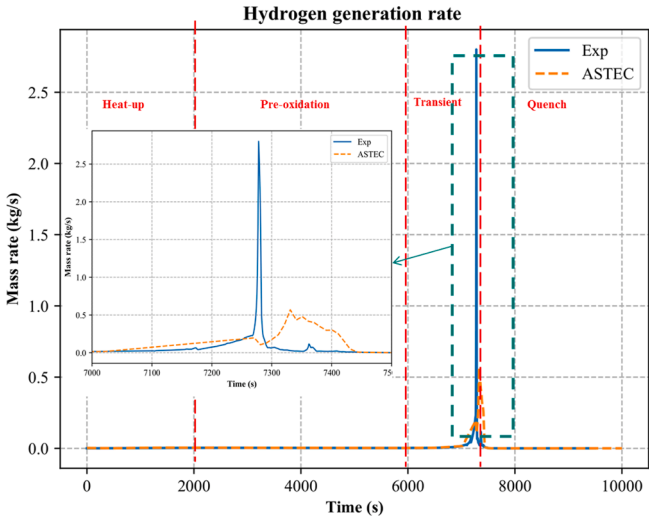

Fig. 28. Hydrogen production rate in time.

hydrogen generation at the end of transient was compared to the test data. Total hydrogen production estimated by ASTEC was about 83 g which 35 g is generated before quenching phase. This amount was 1.5 times higher than the experiment which was measured as 58 g, during the re-flood 25 g was released (Stuckert et al., 2008). There it can be observed that ASTEC over-predicts the hydrogen generation during the pre-quench phases while the shape of both measured data and predicted data is similar. However, during quench phase, the hydrogen generation was far over-predicted by ASTEC. One explanation to it may be the higher hydrogen absorption of E110 and E250 (Hózer et al., 2008) (Hózer et al., 2005). Since these materials absorb more hydrogen, it would decrease produced hydrogen before quench phase. Higher temperatures at the quenching phase may result higher amount of hydrogen generation during breakaway phase. Furthermore, models for hydrogen release which are developed for Zr-4 could be insufficient to estimate breakaway oxidation parameters for VVER-related materials since the breakaway region is different for these materials. But a higher hydrogen production rate is predicted before quenching due to the lower hydrogen uptake of Zr-4.

Fig. 29 and Fig. 30 represent oxide scale on heated and unheated rods and average of oxide scale in experiment data. Estimation for oxide scale at selected specimens is close to experimental average. From Figs. 31 to

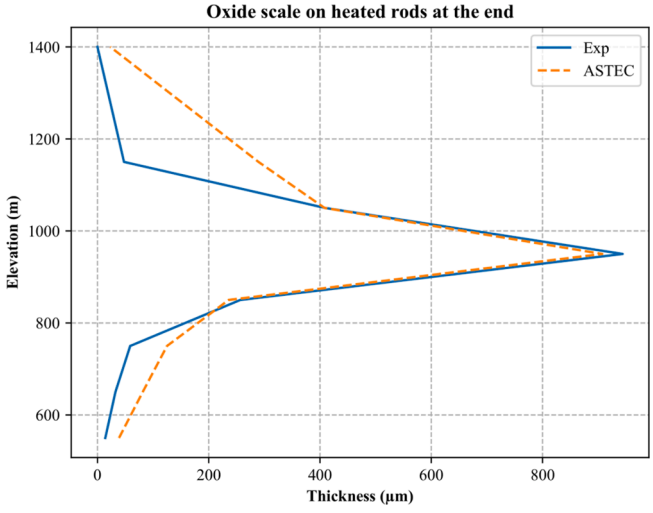

Fig. 29. Oxide scale on heated rods against average oxide scale (Exp) for heated rods.

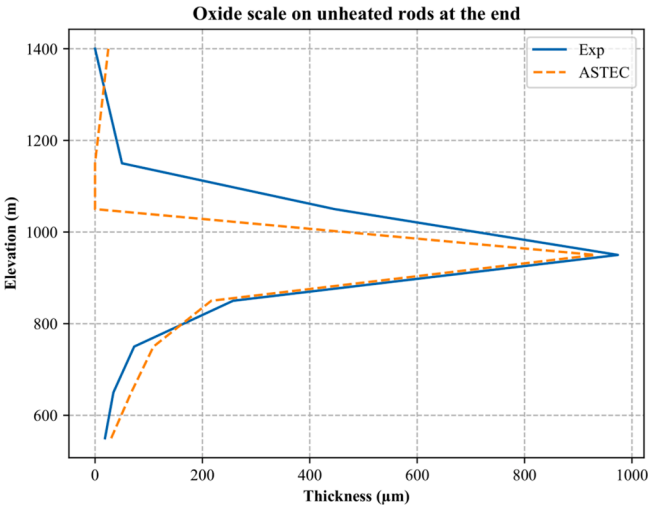

Fig. 30. Oxide scale on unheated rods against average oxide scale (Exp) for unheated rods.

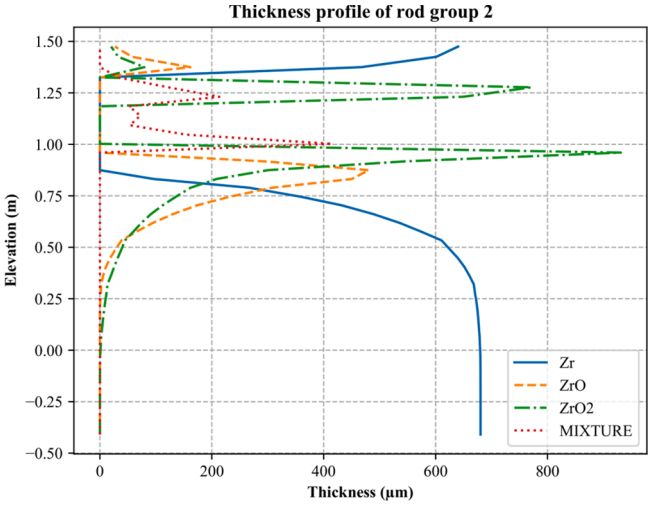

Fig. 31. Thickness profile of inner heated rods.

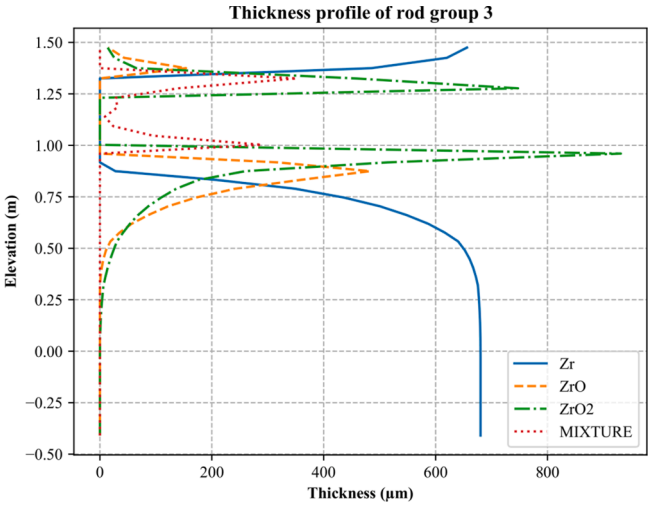

Fig. 32. Thickness profile of inner unheated rods.

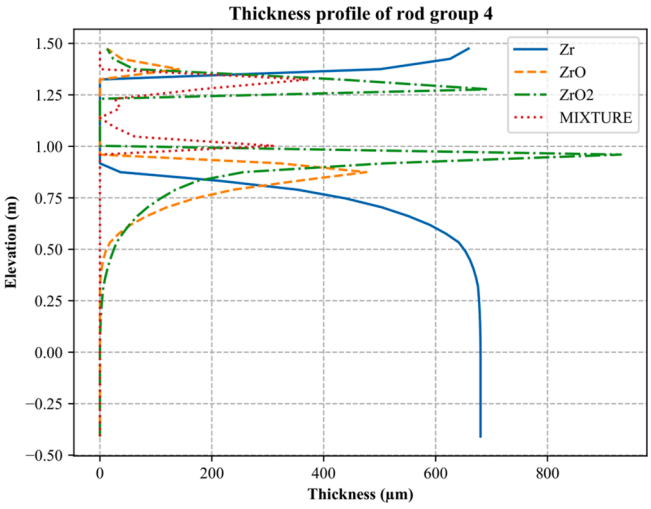

Fig. 33. Thickness profile of outer unheated rods.

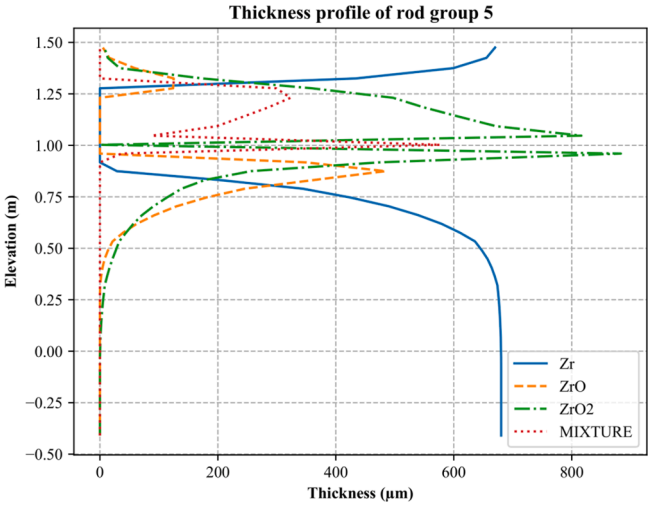

Fig. 34. Thickness profile of outer heated rods.

34 show the oxidation profile of selected rod group at the end of experiment. The model calculates oxide scale starting from Zr and estimates physio-chemical process of clad structures. As seen from figures, meltdown of materials was observed in model as in experiment. Zr and ZrO scales are depleted especially around 950 mm which is the location of break. In the experiment, the meltdown has been observed at 950 mm for each rod group which ASTEC estimated the meltdown of cladding surface at these elevations.

Temperature profile results for all rod groups and shroud area is in great coherence with experiment. Estimation of higher temperature than experiment at 950 mm can lead to higher oxidation. Meshing of model at this elevation was not exactly on 950 mm, therefore, taking average of upper and lower meshes around 950 mm would create some differences. All curves show qualitatively similar global trends over all test phases. Since thermal properties of Zr-4 and E110 or E250 until the break-away phase are similar, it is expected to obtain temperatures close to experiment. The thermocouples attached to the cladding surface affect the flow area. Therefore, it should be noted that there are difference in temperatures measured in thermocouples at same elevation up to ∓ 80 K.

The temperature difference between QUENCH-06 and QUENCH-12 cladding temperatures were reported as 30–40 K so using Zr-4 instead of Zr-1%Nb and Zr-2.5%Nb can be the reason of decrease (Stuckert et al., 2008). Additionally, different material usage could lead

differences on the oxide scale estimations for the rods ejected during the test and at the end of the test.

Similar results and similar missing phenomena like implementation of oxidation models for E110 and E250 were reported for applications on different codes (Palagin and Stuckert, 2007; Georgiev and Stuckert, 2012). However, developed model was able to model break-away oxidation phenomena of clad structures and rapid increase of oxidation and hydrogen generation due to rapid steam existing environment, oxidation of corner rod structures like experiment (Stuckert et al., 2008) and later break-away oxidation of VVER QUENCH-12 clad structures than PWR QUENCH-06 clad structures. The oxidation model used in the simulation was not able to completely predict the higher E110 and E250 hydrogen absorption due to their thermo-physical and chemo-physical characteristics. Also modelling transient with all corner rods inside of core which some of them are ejected in experiment, made temperature estimations lower since flow area should be decreased in the modelling. Despite the all assumption, ASTEC code was able to predict temperatures reasonably and able to show and consider many phenomena like oxidation and chemical processes.

4. Conclusions

In this work, QUENCH-12 experiment, which is oxidation and hydrogen generation test of VVER specific materials Zr-1%Nb (E110) and Zr-2.5%Nb in severe accident conditions, is modelled with ASTEC integral code and results of estimations are compared with experimental results. Capabilities of ASTEC code were tested against the experiment and validation of ASTEC code for VVER reactors has been done.

Based on the simulations performed with ASTEC V2 it can be concluded that the QUENCH-12 tests was satisfactorily analyzed despite the use of Zr-4 instead of the VVER-specific material used in the test for the cladding, the shroud and the corner rods. The generated hydrogen estimated as 83 g which 35 g of hydrogen are produced during quenching phase. In experiment of QUENCH-12, generated hydrogen measured as 58 g and 24 g of this measured at reflooding stage. This difference may be resulted from the lack of VVER-specific data (E110 and E250 material) in the ASTEC-databank. The temperature of the simulator rods, shroud and corner rods at 950 mm elevation are in good agreement with the data.

In the future, the temperature dependent thermo-physical properties for the specific material used in the test need e.g. E110 and E250 have to be used to improve the simulation results. It is worth to note that the oxidation models are developed based on tin enriched materials. However, E110 and E250 is niobium enriched cladding materials with 1% and 2.5% of Niobium. This validation work also will be a milestone for further full-plant VVER analysis and severe accident modelling.

CRediT authorship contribution statement

Ahmet Kağan Mercan: Writing – original draft, Writing – review & editing, Investigation, Visualization. **V.H. Sánchez-Espinoza:** Writing – review & editing, Methodology, Software. **Fabrizio Gabrielli:** Writing – review & editing, Supervision.

Declaration of Competing Interest

The authors declare that they have no known competing financial interests or personal relationships that could have appeared to influence the work reported in this paper.

Acknowledgments

The authors would like to thank Dr. Stuckert for experimental data and enlightening specific points related with QUENCH tests, ASTEC team under KIT/INR for the assist for development of model and Mr. Chatelard for particular solutions related with ASTEC. The corresponding author is funded by Republic of Turkey Ministry of National Education during his Ph.D. studies.

References

OECD/NEA, 2013. The Fukushima Daiichi Nuclear Power Plant Accident OECD/NEA Nuclear Safety Response and Lessons Learnt. OECD.

BMUB, "German Action Plan for the implemantation of measures after Fukushima Daiichi reactor accident," 2012.

BMUB, "Updated German Action Plan for the implementation of measures after Fukushima reactor accident," 2014.

Kymäläinen, O., Tuomisto, H., Theofanous, T.G., 1997. In-vessel retention of corium at the Loviiase plant. Nucl. Eng. Des. 169, 109–130.

D'Auria, F., Suslov, A., Muellner, N., Petrangeli, G., Cherubini, M., 2008. Accident Management in VVER-1000. Sci. Technol. Nucl. Installations 2008, 1–5.

Chatterjee, B., Mukhopadhyay, D., Lele, H., Atanasova, B., Groudev, P., 2011. Severe accident management strategy verification for VVER-100 (V320) reactor. Nucl. Eng. Des. 241, 3977–3984.

Gencheva, R., Stefanova, A., Groudev, P., 2015. Plant application of ICARE/ASTECv2.0rev3 computer code for investigation of in vessel retention in VVER-1000 reactor design. Ann. Nuclear Energy 81, 207–212.

Kruse, P., Brähler, T., Koch, M.K., 2014. Validation of ASTEC core degradation and containment models. Nucl. Eng. Des. 272, 173–182.

Gonfiotti, B., Paci, S. 2018. Stand-alone containment analysis of Phébus FPT tests with ASTEC and MELCOR codes: the PFT-2 test. *Heliyon* 4(3).

Chatelard, P., Reinka, N. 2009. Overview of the integral code ASTEC V2.0, IRSN.

Chatelard, P., Reinke, N., Arndt, S., Belon, S., Cantrel, L., Carenini, L., Chevalier-Jabet, K., Cousin, F., Eckel, J., Jacq, F., Marchetto, C., Mun, C., Piar, L., 2014. ASTEC V2 severe accident integral code main features, current V2.0 modelling status, perspectives. Nucl. Eng. Des. 272, 119–135.

Chatelard, S. B. L. B. L. C. O. C. F. C. C. M. H. N. L. P. L. C. P. 2016. Main modelling features of the ASTEC V2.1 major version. *Ann. Nuclear Energy* 93(0306-4549), 83-96.

Fichot, F., Carénini, L., Sangiorgi, M., Hermsmeyer, S., Miassoedov, A., Bechta, S., Zdarek, J., Guennadou, D. 2017. Status of the IVMR project: First steps towards a new methodolgy to assess In-Vessel Retention strategy for high-power reactors. in *8th European Review Meeting on Severe Accident Research (ERMSAR)*, Warsaw.

Belon, S., Bouillet, C., Topin, V., Bonneville, H., Andrews, N. 2017. "Insight of core fegradation simulation in integral codes throughout ASTEC/MELCOR crosswalk comparisons and ASTEC sensitivity studies," in *8th European Review Meeting on Severe Accident Research*, Warsaw.

Chatelard, P., Gabrielli, F., Fichot, F., Bonneville, H., Bouillet, C., Belon, S., Chailan, L., Sanchez, V. 2017. Contribution of ASTEC numerical simulations to the understanding of the Fukushima," in *IAEA Workshop on advances in understanding the progression of severe accidents in Boiling Water Reactors*, Vienna.

M. M. A. B. F. M. A. C. S. M. Pietro Maccari. 2021. ASTEC - RAVEN coupling for uncertainty analysis of an ingress of coolant event in fusion plants. *Fusion Eng. Des.* 169(0920-3796).

B. J. F. R. F. A. D. A. G. B. M. B. M. B. D. D. C. R. D. P. D. S. E. L. H. T. H. G. H. A. K. I. K. O. K. T. L. C. L. K. M. P. M. O. Coindreau, 2018. Severe accident code-to-code comparison for two accident scenarios in a spent fuel pool. *Ann. Nucl. Energy* 120 (0306-4549), 880-887.

Henrie, J.O., Postma, A.K., 1987. Lessons Learned from Hydrogen Generation and Burning during the TMI-2 Event. U.S. Department of Energy, USA.

Sehgal, B.R. 2012. Light Water Reactor Safety: A Historical Review, in *Nuclear Safety in Light Water Reactors*, ELSEVIER academic Press, pp. 1-88.

Seopold L.H.P. 2001. Reflooding experiments with LWR-type fuel rod simulators. *Nucl. Eng. Des.* 205-220.

Sepold, L., Hering, W., Homann, C., Miassoedov, A., Schanz, G., Stegmaier, U., Steinbrück, M., Steiner, H., Stuckert, J., 2004. Experiemental and Computational Results of the QUENCH-06 Test (OECD ISP-45). Forschungszentrum Karlsruhe in der Helmholtz-Gemeinschaft, Karlsruhe.

Palagin, A.V., Stuckert, J., 2007. Application of the SVECHA/QUENCH Code to the Simulation of the Bundle Tests QUENCH-06 and QUENCH-12. Forschungzentrum Karlsruhe in der Helmhotz-Gemeinschaft, Karlsruhe.

Georgiev, Y.G., Stuckert, J., 2012. Analysis of the QUENCH-12 bundle experiment with ATHLET-CD2.2A code. KIT Scientific Publishing, Karlsruhe.

Stuckert, J., Goryachev, A., Große, M., Heck, M., Ivanova, I., Schanz, G., Sepold, L., Stegmaier, U., Steinbrück, M., 2008. Results of the QUENCH-12 Experiment on Reflood of a VVER-type Bundle. Forschungzentrum Karlsruhe in der Helmholtz-Gemeinschaft, Karlsruhe.

Volchek, A., Zvonarev, Y., Schanz, G., 2004. Advanced treatment of zircaloy cladding high-temperature oxidation in severe accident code calculations PART II. Best Fitted parabolic correlations. Nucl. Eng. Des. 232 (1), 85–96.

Research Intitute of Atomic Reactors (RIAR), "Annual Report of 2018," Research Intitute of Atomic Reactors (RIAR), Dimitrovgrad, 2019.

Karlsruhe Institute of Technology (KIT), "Annual Report 2020 of Karlsruhe Institute of Technology," Karlsruhe Institute of Technology (KIT), Karlsruhe, 2020.

Hózer, Z., Győri, C., Matus, L., Horváth, M., 2008. Ductile-to brittle transition of oxidised Zircaloy-4 and E110 claddings. J. Nucl. Mater. 373 (1-3), 415–423.
Hózer, Z., Gyuöri, C., Horváth, M., Nagy, I., Maróti, L., Matus, L., Windberg, P., Frecska, J., 2005. Ballooning experiments with VVER claddings. Nucl. Technol. 152 (3), 273–285.
Gómez-García-Toraño, I., Sánchez-Espinoza, V.-H., Stieglitz, R., Stuckert, J., Laborde, L., Belon, S., 2017. Validation of ASTECV2.1 based on the QUENCH-08 experiment. Nucl. Eng. Des. 314, 29–43.